Studies with H-2K^b cells

H-2K^b cells derived from the muscle of heterozygous H-2K^b-ts-A58 transgenic mice[17] were differentiated[18] and transfected with adenovirus containing control vector or dominant-negative AMPK[16]. Five days later, cells were treated with leptin (100 nM) for 2 h in HEPES-buffered saline containing 5 mM glucose, and the AMPK activity and phosphorylation of ACC were examined.

Measurement of catecholamine and AMP, ADP, ATP content

Soleus muscles were homogenized with 0.5 N perchloric acid and centrifuged. We measured total catecholamine content in the supernatant by a radioenzymatic assay kit (Amersham Pharmacia). AMP, ADP and ATP were determined by anion exchange chromatography using a SMART system (Amersham Pharmacia)[28].

Western blot analysis

Phosphorylation of the α-subunit of AMPK and ACC in soleus lysates (40 μg of protein) was determined with 4–15% gradient SDS acrylamide gels using antibodies against phosphopeptides based on the amino-acid sequence surrounding Thr 172 of the α-subunit of human AMPK (Cell Signaling) and Ser 79 of rat ACC (Upstate Biotech.). We determined protein levels of α2 AMPK and ACC by using a specific antibody for the α2 subunit of AMPK (ref. 24) and streptavidin–horseradish peroxidase (Amersham Pharmacia)[29], respectively.

Statistical analysis

All values are the mean ± s.e.m.. Data were evaluated by factorial analysis of variance and Newman–Keuls multiple range test. The difference was considered to be significant if $P < 0.05$.

Received 28 August; accepted 12 October 2001.

1. Friedman, J. M. & Halaas, J. L. Leptin and the regulation of body weight in mammals. *Nature* **395,** 763–770 (1998).
2. Muoio, D. M. *et al.* Leptin directly alters lipid partitioning in skeletal muscle. *Diabetes* **46,** 1360–1363 (1997).
3. Kamohara, S., Burcelin, R., Halaas, J. L., Friedman, J. M. & Charron, M. J. Acute stimulation of glucose metabolism in mice by leptin treatment. *Nature* **389,** 374–377 (1997).
4. Minokoshi, Y., Haque, M. S. & Shimazu, T. Microinjection of leptin into the ventromedial hypothalamus increases glucose uptake in peripheral tissues in rats. *Diabetes* **48,** 287–291 (1999).
5. Unger, R. H., Zhou, Y.-T. & Orci, L. Regulation of fatty acid homeostasis in cells: novel role of leptin. *Proc. Natl Acad. Sci. USA* **96,** 2327–2332 (1999).
6. Hardie D. G., Carling, D. & Carlson, M. The AMP-activated/SNF1 protein kinase subfamily: metabolic sensors of the eukaryotic cell? *Ann. Rev. Biochem.* **67,** 821–855 (1998).
7. Winder, W. W. & Hardie, D. G. AMP-activated protein kinase, a metabolic master switch: possible roles in type 2 diabetes. *Am. J. Physiol.* **277,** E1–E10 (1999).
8. Kahn, B. B. & Flier, J. S. Obesity and insulin resistance. *J. Clin. Invest.* **106,** 473–481 (2000).
9. Ruderman, N. B., Saha, A. K., Vavvas, D. & Witters, L. A. Malonyl-CoA, fuel sensing, and insulin resistance. *Am. J. Physiol.* **276,** E1–E18 (1999).
10. Lee, Y. *et al.* Liporegulation in diet-induced obesity. The antisteatotic role of hyperleptinemia. *J. Biol. Chem.* **276,** 5629–5635 (2001).
11. Schwartz, M. W., Woods, S. C., Porte, D. Jr, Seeley, R. J. & Baskin, D. G. Central nervous system control of food intake. *Nature* **404,** 661–671 (2000).
12. Abu-Elheiga, L., Matzuk, M. M., Abo-Hashema, K. A. H. & Wakil, S. J. Continuous fatty acid oxidation and reduced fat storage in mice lacking acetyl-CoA carboxylase 2. *Science* **291,** 2613–2616 (2001).
13. Stein, S. C., Woods, A., Jones, N. A., Davison, M. D. & Carling, D. The regulation of AMP-activated protein kinase by phosphorylation. *Biochem. J.* **345,** 437–443 (2000).
14. Ponticos, M. *et al.* Dual regulation of the AMP-activated protein kinase provides a novel mechanism for the control of creatine kinase in skeletal muscle. *EMBO J.* **17,** 1688–1699 (1998).
15. Higaki, Y., Hirshman, M. F., Fujii, N. & Goodyear, L. J. Nitric oxide increases glucose uptake through a mechanism that is distinct from the insulin and contraction pathways in rat skeletal muscle. *Diabetes* **50,** 241–247 (2001).
16. Woods, A. *et al.* Characterization of the role of AMP-activated protein kinase in the regulation of glucose-activated gene expression using constitutively active and dominant negative forms of the kinase. *Mol. Cell. Biol.* **20,** 6704–6711 (2000).
17. Jat, P. S. *et al.* Direct derivation of conditionally immortal cell lines from an H-2K^b-ts-A58 transgenic mouse. *Proc. Natl. Acad. Sci. USA* **88,** 5096–5100 (1991).
18. Fryer, L. G. D. *et al.* Activation of glucose transport by AMP-activated protein kinase via stimulation of nitric oxide synthase. *Diabetes* **49,** 1978–1985 (1999).
19. Haynes, W. G., Morgan, D. A., Walsh, S. A., Mark, A. L. & Sivitz, W. I. Receptor-mediated regional sympathetic nerve activation by leptin. *J. Clin. Invest.* **100,** 270–278 (1997).
20. Kishi, K. *et al.* AMP-activated protein kinase is activated by the stimulations of G_q-coupled receptors. *Biochem. Biophys. Res. Commun.* **276,** 16–22 (2000).
21. Martin, W. H, Tolley, T. K. & Saffitz, J. E. Autoradiogaraphic delineation of skeletal muscle α_1-adrenergic receptor distribution. *Am. J. Physiol.* **259,** H1402–H1408 (1990).
22. Akaike, N. Sodium pump in skeletal muscle: central nervous system-induced suppression by α-adrenoreceptors. *Science* **213,** 1252–1254 (1981).
23. Stafford I. L. & Jacobs, B. L. Noradrenergic modulation of the masseteric reflex in behaving cats. I. Pharmacological studies. *J. Neurosci.* **10,** 91–98 (1990).
24. Woods, A., Salt, I., Scott, J., Hardie, D. G. & Carling, D. The α1 and α2 isoforms of the AMP-activated protein kinase have similar activities in rat liver but exhibit differences in substrate specificity *in vitro*. *FEBS Lett.* **397,** 347–351 (1996).
25. Hayashi, T. *et al.* Metabolic stress and altered glucose transport. Activation of AMP-activated protein kinase as a unifying coupling mechanism. *Diabetes* **49,** 527–531 (2000).
26. Goodwin, G. W. & Taegtmeyer, H. Regulation of fatty acid oxidation of the heart by MCD and ACC during contractile stimulation. *Am. J. Physiol.* **277,** E772–E777 (1999).
27. Oakes, N. D. *et al.* Development and initial evaluation of a novel method for assessing tissue-specific plasma free fatty acid utilization *in vivo* using (*R*)-2-bromopalmitate tracer. *J. Lipid. Res.* **40,** 1155–1169 (1999).
28. Corton, J. M., Gillespie, J. G. & Hardie, D. G. Role of the AMP-activated protein kinase in the cellular stress response. *Curr. Biol.* **4,** 315–324 (1994).
29. Vavvas, D. *et al.* Contraction-induced changes in acetyl-CoA carboxylase and 5′-AMP-activated kinase in skeletal muscle. *J. Biol. Chem.* **272,** 13255–13261 (1997).

Acknowledgements

We thank N. D. Oakes for the gift of [9,10-^{3}H]-(*R*)-2-bromopalmitate, and B. B. Lowell and L. A. Witters for helpful advice. This work was supported by NIH grants (B.B.K.), the Boston Obesity Nutrition Research Center (Y.-B.K.), and The Kato Memorial Trust for Nambyo Research and Mitsui Life Social Welfare Foundation (Y.M.).

Correspondence and requests for materials should be addressed to B.B.K. (e-mail: bkahn@caregroup.harvard.edu).

Energetic landscape of α-lytic protease optimizes longevity through kinetic stability

Sheila S. Jaswal*, Julie L. Sohl, Jonathan H. Davis* & David A. Agard

Howard Hughes Medical Institute and the Department of Biochemistry and Biophysics, University of California at San Francisco, San Francisco, California 94143-0448, USA

During the evolution of proteins the pressure to optimize biological activity is moderated by a need for efficient folding. For most proteins, this is accomplished through spontaneous folding to a thermodynamically stable and active native state. However, in the extracellular bacterial α-lytic protease (αLP) these two processes have become decoupled. The native state of αLP is thermodynamically unstable, and when denatured, requires millennia ($t_{1/2} \sim 1{,}800$ years)[1] to refold. Folding is made possible by an attached folding catalyst, the pro-region, which is degraded on completion of folding, leaving αLP trapped in its native state by a large kinetic unfolding barrier ($t_{1/2} \sim 1.2$ years)[1]. αLP faces two very different folding landscapes: one in the presence of the pro-region controlling folding, and one in its absence restricting unfolding. Here we demonstrate that this separation of folding and unfolding pathways has removed constraints placed on the folding of thermodynamically stable proteins, and allowed the evolution of a native state having markedly reduced dynamic fluctuations. This, in turn, has led to a significant extension of the functional lifetime of αLP by the optimal suppression of proteolytic sensitivity.

αLP and virtually all other extracellular bacterial proteases are synthesized with a pro-region and where examined, the pro-regions are required for folding of the attached protease[2]. Thus, many of these other proteases are expected to share the unusual features of folding energetics of αLP. The biological function of secreted bacterial proteases is to provide nutrients for the bacterium. As they function in the soil, there is no need for their regulated turnover. Therefore the native states of these proteases are likely to be highly optimized for survival under harsh, highly proteolytic conditions. We have investigated the possibility that αLP—and

* Present addresses: Department of Molecular Biophysics and Biochemistry, Yale University, New Haven, Connecticut 06520-8114, USA (S.S.J.); Lexigen Pharmaceuticals, 125 Hartwell Avenue, Lexington, Massachusetts 02421, USA (J.H.D.).

probably other pro-proteases and proteins functioning under extreme conditions—has evolved kinetic stability via unique native-state properties in addition to the large unfolding barrier[1] (Fig. 1), as a means to achieve optimal proteolytic resistance, thereby extending biological function.

This proposal raises the question of how native-state properties arising from kinetic stability lead to effective protease resistance. As between four and eight residues of the substrate peptide chain are required to fit in a precise manner into the deep cleft that forms the protease active site[3], flexible regions of a protein are the most accessible targets for proteolysis[4]. Even proteins lacking proteolytically accessible flexible loops in their native states are conformationally dynamic, constantly sampling open, proteolytically vulnerable conformations in processes ranging from small breathing motions to global unfolding: a finding that has been well established from native-state hydrogen exchange studies[5,6]. Thus, proteolytic degradation can be described by the following conformational equilibrium reaction[7,8]:

$$\text{Native} \underset{\text{Closing}}{\overset{\text{Opening}}{\rightleftharpoons}} \text{Open/protease accessible} \xrightarrow{\text{Cleavage}} \text{Cleaved}$$

Therefore, to optimally avoid proteolytic attack and prolong its lifetime, a protein must not only eliminate native-state proteolysis but also restrict those unfolding and dynamic opening events leading to protease accessibility.

To test whether αLP shows restricted native-state dynamics in addition to its severely restricted global unfolding[1], we assessed the ability of water to penetrate the protease by hydrogen–deuterium exchange (H–X) monitored by two-dimensional nuclear magnetic resonance (NMR) spectroscopy. H–X is a sensitive and residue-specific probe of conformational fluctuations based on the rate at which amide protons exchange with solvent deuterons[6]. Amide protons buried in the core of a protein are protected from solvent exchange. The degree of protection from exchange is quantified using protection factors (P_f) corresponding to the ratio of the intrinsic exchange rate (k_{int}) of the solvent-exposed amide to the observed exchange rate (k_{obs}): $P_f = k_{int}/k_{obs}$. Protons on the surface or in dynamic regions of the protein sampling partially unfolded conformations exchange much more rapidly and have lower P_f values than those in rigid regions of the protein.

As shown in Fig. 2, αLP displays extremely high protection from H–X across the entire molecule. Although most proteins typically display a 'slow exchange core'[9] of only 3–8 residues with their highest P_f values ranging from 10^4 to 10^8, more than half of the amide protons of αLP (103) have P_f values greater than 10^4. Notably, 31 of those amide protons display P_f values greater than 10^9; 18 are so highly protected that no exchange was measured at all, even after six months at pH 9, corresponding to P_f values of $>10^{9.4}$ to $10^{10.7}$. Not only is this degree of protection among the highest to be measured in a protein[10], but the most slowly exchanging residues are spread throughout both domains of the protein instead of being localized to one discrete 'core', as is usually seen. Therefore αLP has a conformational rigidity well beyond that seen for traditional, thermodynamically stabilized proteins.

The high degree of rigidity observed by H–X extends previous thermodynamic measurements demonstrating that the native state of αLP is enthalpically favoured over its partially unfolded intermediate by 18 kcal mol^{-1} (ref. 1), and as a consequence, its thermodynamic instability must derive from an excessive loss in entropy during the course of folding. A possible source for this unusually large entropy decrease is the high number of glycines found in the sequence of αLP and all other pro-region-containing members of the chymotrypsin family (18% on average compared with 9% in

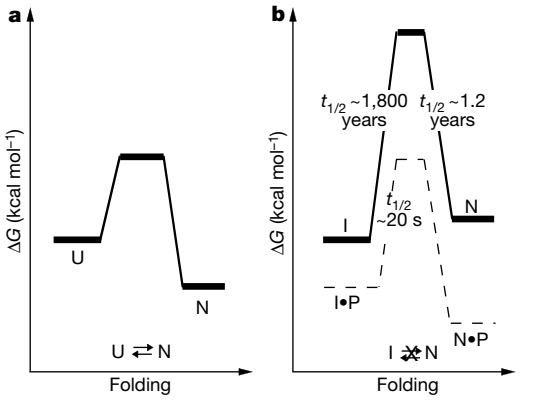

Figure 1 Folding free-energy diagrams for thermodynamic compared with kinetic stability. ΔG, free energy difference. **a**, A typical protein that folds on its own to a thermodynamically stable native state (N) is in equilibrium with its unfolded states (U), therefore it is constantly sampling protease-accessible conformations. **b**, In the absence of the pro-region (solid line) the large barrier prevents the native state of αLP (N) from being in equilibrium with the more stable intermediate (I) and other unfolded conformations. In the presence of the pro-region (P; dashed line) the barrier is lowered and N is stabilized. Refolding rates were determined by measuring an increase in αLP activity owing to formation of N over time during incubation of I in the absence or presence of pro[1]. The unfolding rate was determined from fluorescence measurements of inactive S195A αLP unfolded in varying amounts of denaturant and extrapolated to water[1]. Experiments were performed at 4 °C, pH 5.0 (ref. 1).

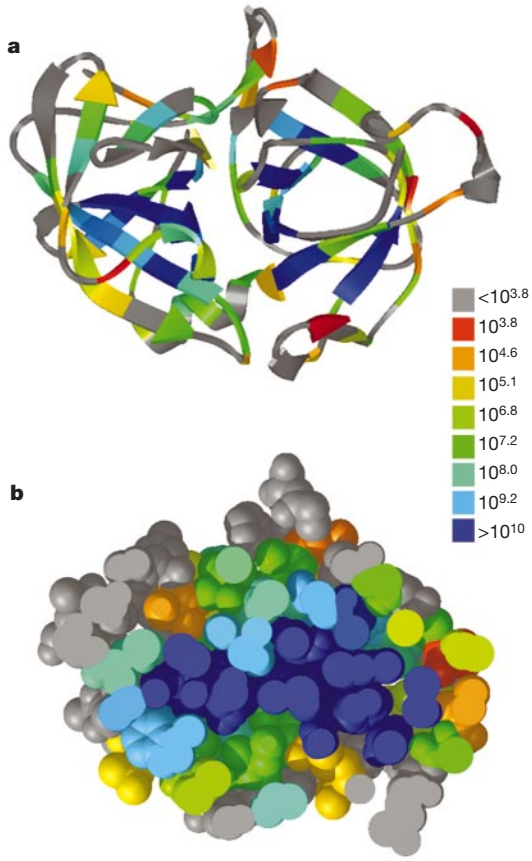

Figure 2 Hydrogen-exchange protection of αLP. **a**, **b**, Ribbon (**a**) and space-filling (**b**) representations of αLP coloured by amide protection factors. Residues with amide protection factors $<10^{3.8}$ are coloured grey. Residues with protection factors of $10^{3.8}$ to $\geq 10^{10.7}$ are coloured from red to blue. (A table listing the calculated protection factors at each pH is included as Supplementary Information.) The entire protease molecule is shown in **a**. A slice through the middle of the molecule in **b** reveals protection patterns in its interior. Figures were generated using MIDAS[24].

Table 1 Survival assay rates

pH	Protease	Inactivation rate (day^{-1})	Cleavage rate (day^{-1})
5	αLP	0.005 ± 0.001	0.01 ± 0.002
5	Trypsin	0.5 ± 0.02	0.29 ± 0.05
5	Chymotrypsin	0.06 ± 0.01*	0.072 ± 0.05*
7	αLP	0.006 ± 0.001	0.009 ± 0.007
7	Trypsin	0.83 ± 0.05	0.8 ± 0.2
7	Chymotrypsin	1.43 ± 0.08	0.9 ± 0.1
8	αLP	0.003 ± 0.001	ND
8	Trypsin	0.62 ± 0.05	ND
8	Chymotrypsin	2.22 ± 0.07	ND

Inactivation values indicate the rate of loss of enzyme activity on chromogenic substrate. Cleavage values indicate the rate of loss of a band on gel. The pH independence of the rate of αLP inactivation indicates that the unimolecular unfolding reaction is rate-limiting (see text), not the bimolecular cleavage reaction. ND, not determined.
*Chymotrypsin dimerizes at pH 5 (ref. 23), leading to an anomalously slow rate of inactivation (see data at pH 7 and 8 for typical behaviour).

homologues lacking pro-regions)[1]. High glycine content would increase the entropy of unfolded states, but could also lead to greater native-state rigidity and increased proteolytic resistance by allowing tighter turns and tighter packing.

To assess whether the unusual dynamic properites of αLP sufficiently restrict conformational fluctuations to enhance proteolytic stability, we directly compared the lifetimes of αLP and its thermodynamically stabilized[11,12] mammalian homologues, chymotrypsin and trypsin, under highly proteolytic conditions. Survival assays were set up in which equimolar amounts of all three proteases were mixed and incubated at pH 5, 7 and 8, providing a nearly 1,000-fold variation in proteolytic activity. Because the substrate specificities of the enzymes are orthogonal, it was possible to assay the survival of each protease over time by measuring the enzymatic activity of the mixture on three different chromogenic substrates, specific for each protease. The biological activity of αLP remains virtually unchanged, whereas its mammalian counterparts are readily destroyed at rates ≥100-fold faster than αLP (Fig. 3a and Table 1). This is not due to a greater number of, or increased accessibility to, proteolytic sites on chymotrypsin and trypsin. In fact, when normalized to the number of residues, αLP has the same percentage of sites (defined as ≥20% surface accessibility) as chymotrypsin and ~30% more than trypsin. Nor is the longer lifetime of αLP due to an ability to remain active when cleaved. At pH 7, the rates of cleavage monitored by gel electrophoresis for all three proteases are within twofold of their inactivation rates (Fig. 3b and Table 1). Therefore, αLP has the ability to withstand proteolysis and autoproteolysis for months longer than its thermodynamically stabilized counterparts.

We next determined whether αLP has a protease resistance that is optimized to the greatest extent possible. Given the very slow rate of αLP global unfolding[1], the most sensitive measure of optimization for proteolytic resistance is whether local unfolding transitions that could lead to proteolysis at a faster rate than through global unfolding have also been suppressed. This was examined quantitatively by comparing the rate of inactivation of αLP through autoproteolysis, measured by loss of enzymatic activity, to its rate of global unfolding in the absence of proteolysis, measured by following the fluorescence decrease during unfolding of an inactive variant, S195A αLP (active site Ser replaced by Ala) (Fig. 4). The rate of αLP autoproteolysis is 0.04 day^{-1}; the global unfolding rate is 0.02 day^{-1}. The twofold difference in rate may be due to a greater stability of the variant, but in any case corresponds to a free-energy difference of only 0.3 kcal mol^{-1}. This indicates that the extraordinary rigidity at the molecular level demonstrated by H–X successfully restricts local unfolding fluctuations so that only global unfolding, which occurs on a year timescale, leads to proteolytic accessibility.

These results provide the first functional rationale, to our knowledge, for the existence of pro-region-dependent folding. The observed suppression of both local and global unfolding transitions must be the direct consequence of an almost perfectly cooperative barrier to unfolding. Such extreme cooperativity comes at a significant energetic cost: the native state of αLP is not thermodynamically stable and can be reached only with the help of its pro-region. Thus, the development of desirable native-state properties has been made possible only by the transient existence of the pro-region, which has allowed the energetic landscape of the native state to evolve independently of the folding landscape.

Kinetic stability provides a novel mechanism for the evolution of optimal functional properties. When coupled with pro-region-dependent folding it provides for enhanced longevity in degradatory environments not only for αLP, but probably for a wide array of pro-region-containing proteases and other secreted enzymes. In addition, kinetic stability can function as a timer to regulate biological function in non-proteolytic proteins that have an efficient folding pathway[13]. Examples include serpins[14], membrane fusion proteins such as influenza haemagglutinin[15,16] and possibly HIV gp41 (ref. 17), and heat-shock transcription factor[18]. Kinetic stability is also a fundamental aspect of many human amyloid diseases, in

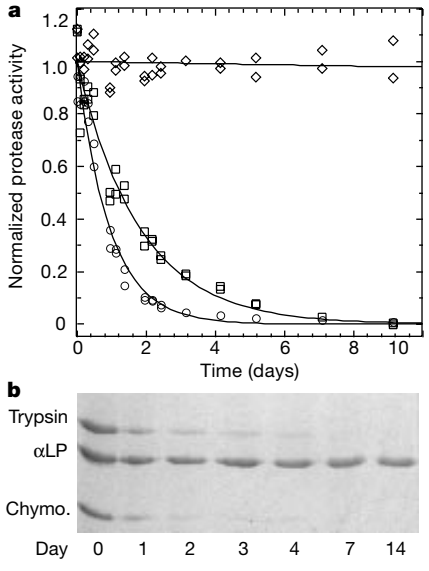

Figure 3 Survival assay at pH 7, 25 °C. **a**, αLP (diamonds) is more resistant to proteolysis than chymotrypsin (circles) and trypsin (squares), as monitored by loss of proteolytic activity of the mixture on three different chromogenic substrates specific for each protease. **b**, Quantification of the loss of intact protein monitored by SDS–polyacrylamide gel electrophoresis.

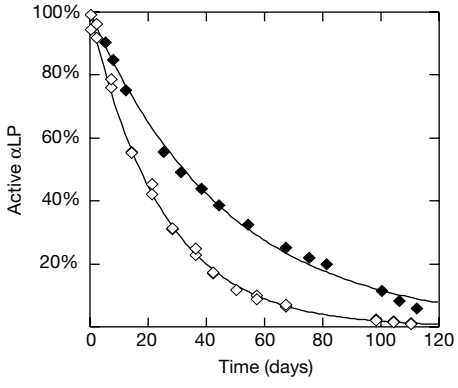

Figure 4 Autolysis compared with global unfolding rate. At 25 °C, 1 M GdnHCl, where local unfolding is promoted, the rate of autoproteolysis of the active enzyme (open symbols) monitored by loss of proteolytic activity is less than twofold faster than the rate of global unfolding of the inactive enzyme (filled symbols) monitored by loss of fluorescence.

which a barrier separating the native conformation from an inactive or even toxic conformation is surmounted over time or lowered through mutation or perturbed conditions[19]. The use of kinetic stability highlights the importance of the role of protein-folding energetics and dynamics, beyond simply specifying the active conformation, in critically influencing biological activity and lifetime. □

Methods

Protein expression and purification

αLP and S195A αLP were expressed in *Escherichia coli* and purified as described[1,20] . Rat trypsinogen was expressed in *Pichia* as described[21]. Secreted protein auto-activated to trypsin, which was purified as follows. All buffers contained 10 mM calcium chloride. The supernatant from cells was slowly brought to 4.5 M NaCl, loaded onto a phenyl sepharose fast-flow column, washed with 50 mM MES at pH 6.0, 4.5 M NaCl then eluted with 50 mM MES at pH 6.0. After dialysing to remove NaCl, the eluted protein was loaded onto a p-amino benzamidine agarose column, washed with 50 mM Tris at pH 7.5 and eluted with 100 mM acetic acid into fractions containing 1/20 volume 0.5 M sodium citrate at pH 4.5. Fractions with active protein were pooled and dialysed into 1 mM HCl and assayed for activity as described[21].

Hydrogen exchange

Amide exchange of wild-type αLP was initiated by the addition of protonated 15N-labelled protease to one of the following buffers containing >97% D2O: 100 mM $NaPO_4$, 100 mM NaCl and 2.5 mM NaOAc(d3) at pH 6.84; 100 mM Tris (deuterated), 100 mM NaCl and 2.5 mM NaOAc(d3) at pH 8.04; or 100 mM $NaBO_3$, 100 mM NaCl and 2.5 mM NaOAc(d3) at pH 9.17. Exchange occurred at room temperature and was monitored over a period of 6 months by two-dimensional HSQC (heteronuclear single-quantum correlation spectroscopy) experiments using a Varian 600 MHz NMR spectrometer. Fit peak heights were taken from the processed data and used to calculate the observed exchange rates for each amide proton using a single decaying exponential function. The observed rates were converted into protection factors for each amide using calculated intrinsic exchange rates[22]. Amide assignments at high pH were confirmed by comparing the NOESY (nuclear Overhauser enhancement spectroscopy) crosspeaks with those from a lower pH spectrum. The minimum observable exchange rate was 0.004 day^{-1}. Amides with exchange rates measured at several pH values demonstrated expected EX2 pH dependencies[6], with the exception of five amides, four of which cluster near the active site. A full table of exchange rates as a function of pH is included as Supplementary Information.

Survival assays

A concentration of 6.5 μM αLP, trypsin and chymotrypsin (TLCK (tosyl-L-lysine chloromethyl ketone)-treated; Worthington) were incubated together at 25 °C in 10 mM $CaCl_2$ and 50 mM KOAc pH 5.0, 50 mM MOPS at pH 7, 50 mM HEPES at pH 7, or 50 mM Tris at pH 8. Aliquots were removed over time and the survival of the individual proteases was measured on the basis of their activities, which could be distinguished given their non-overlapping specificities for different substrates (succinyl-Ala-Pro-Ala-pNA, succinyl-Ala-Ala-Pro-Arg-pNA, succinyl-Ala-Ala-Pro-Leu-pNA, used for αLP, trypsin and chymotrypsin, respectively, all substrates at 1 mM in 10 mM $CaCl_2$, 100 mM Tris at pH 8). Cleavage of the proteases during survival assays was monitored by quantifying the disappearance of the full-length species as monitored by band intensity in an SDS–polyacrylamide gel stained with Coomassie, using ImageQuant for Macintosh v1.2.

The inactivation rate (k) in three separate experiments at each pH, and cleavage in single experiments at pH 5 and pH 7 were fit for each protease with a single exponential equation $y = a - b\exp(-kt)$. To normalize for slight concentration variations in separate survival assays, the raw data were treated by subtracting the offset (a) and dividing by the amplitude of the decrease (b). The normalized data from three separate survival assays for each protease at each pH were combined and fit with the single exponential equation to determine the inactivation rate and standard error given in Table 1.

Autolysis assay

αLP (3.25 μM) was incubated in 1 M guanidinium (Gdn)HCl, 10 mM KOAc, pH 5.0, at 25 °C. αLP activity was followed by monitoring the level of hydrolysis of 1 mM succinyl-Ala-Pro-Ala-pNA in 100 mM Tris at pH 8.0 by aliquots removed over time.

Global unfolding

Fluorescence measurements of the inactive mutant S195A αLP at 1.75 μM in 0.98 M GdnHCl, 10 mM KOAc at pH 5.0 were made with excitation at 283 nm, emission 322 nm in an 8100SLM-Aminco fluorimeter connected to an external waterbath set to 25 °C. The sealed fluorescence cuvette was maintained between measurements in a 25 °C incubator.

Received 2 August; accepted 6 November 2001.

1. Sohl, J. L., Jaswal, S. S. & Agard, D. A. Unfolded conformations of α-lytic protease are more stable than its native state. *Nature* **395,** 817–819 (1998).
2. Baker, D., Shiau, A. K. & Agard, D. A. The role of pro regions in protein folding. *Curr. Opin. Cell Biol.* **5,** 966–970 (1993).
3. Perona, J. J. & Craik, C. S. Structural basis of substrate specificity in the serine proteases. *Protein Sci.* **4,** 337–360 (1995).
4. Fontana, A., Polverino de Laureto, P., De Filippis, V., Scaramella, E. & Zambonin, M. Probing the partly folded states of proteins by limited proteolysis. *Fold Des.* **2,** R17–R26 (1997).
5. Chamberlain, A. K. & Marqusee, S. Touring the landscapes: partially folded proteins examined by hydrogen exchange. *Structure* **5,** 859–863 (1997).
6. Englander, S. W., Sosnick, T. R., Englander, J. J. & Mayne, L. Mechanisms and uses of hydrogen exchange. *Curr. Opin. Struct. Biol.* **6,** 18–23 (1996).
7. Rupley, J. A. Susceptibility to attack by proteolytic enzymes. *Methods Enzymol.* **11,** 905–917 (1967).
8. Wang, L. & Kallenbach, N. R. Proteolysis as a measure of the free energy difference between cytochrome *c* and its derivatives. *Protein Sci.* **7,** 2460–2464 (1998).
9. Li, R. & Woodward, C. The hydrogen exchange core and protein folding. *Protein Sci.* **8,** 1571–1590 (1999).
10. Huyghues-Despointes, B. M., Scholtz, J. M. & Pace, C. N. Protein conformational stabilities can be determined from hydrogen exchange rates. *Nature Struct. Biol.* **6,** 910–912 (1999).
11. Santoro, M. M. & Bolen, D. W. Unfolding free energy changes determined by the linear extrapolation method. 1. Unfolding of phenylmethanesulfonyl α-chymotrypsin using different denaturants. *Biochemistry* **27,** 8063–8068 (1988).
12. Wang, E. C., Hung, S. H., Cahoon, M. & Hedstrom, L. The role of the Cys191-Cys220 disulfide bond in trypsin: new targets for engineering substrate specificity. *Protein Eng.* **10,** 405–411 (1997).
13. Lee, C., Park, S. H., Lee, M. Y. & Yu, M. H. Regulation of protein function by native metastability. *Proc. Natl Acad. Sci. USA* **97,** 7727–7731 (2000).
14. Huber, R. & Carrell, R. W. Implications of the three-dimensional structure of alpha 1-antitrypsin for structure and function of serpins. *Biochemistry* **28,** 8951–8966 (1989).
15. Carr, C. M. & Kim, P. S. A spring-loaded mechanism for the conformational change of influenza hemagglutinin. *Cell* **73,** 823–832 (1993).
16. Bullough, P. A., Hughson, F. M., Skehel, J. J. & Wiley, D. C. Structure of influenza haemagglutinin at the pH of membrane fusion. *Nature* **371,** 37–43 (1994).
17. Chan, D. C., Fass, D., Berger, J. M. & Kim, P. S. Core structure of gp41 from the HIV envelope glycoprotein. *Cell* **89,** 263–273 (1997).
18. Orosz, A., Wisniewski, J. & Wu, C. Regulation of *Drosophila* heat shock factor trimerization: global sequence requirements and independence of nuclear localization. *Mol. Cell. Biol.* **16,** 7018–7030 (1996).
19. Kelly, J. W. Alternative conformations of amyloidogenic proteins govern their behavior. *Curr. Opin. Struct. Biol.* **6,** 11–17 (1996).
20. Mace, J. E. & Agard, D. A. Kinetic and structural characterization of muations of glycine 216 in α-Lytic protease: a new target for engineering substrate specificity. *J. Mol. Biol.* **254,** 720–736 (1995).
21. Halfon, S. & Craik, C. S. Regulation of proteolytic activity by engineered tridentate metal binding loops. *J. Am. Chem. Soc.* **118,** 1227–1228 (1996).
22. Bai, Y., Milne, J. S., Mayne, L. & Englander, S. W. Primary structure effects on peptide group hydrogen exchange. *Proteins* **17,** 75–86 (1993).
23. Bolen, D. W. & Santoro, M. M. Unfolding free energy changes determined by the linear extrapolation method. 2. Incorporation of delta G degrees N-U values in a thermodynamic cycle. *Biochemistry* **27,** 8069–8074 (1988).
24. Midas. The MIDAS display system. *J. Mol. Graph.* **6,** 13–27 (1988).

Supplementary Information accompanies the paper on *Nature*'s website (http://www.nature.com).

Acknowledgements

We thank Y. Shibata for assistance with hydrogen exchange experiments, and J. Harris, T. Baird and C. Craik for assistance with trypsin purification. S.S.J. was supported by a Howard Hughes Medical Institute predoctoral fellowship. Research funding was provided by Howard Hughes Medical Institute.

Competing interests statement

The authors declare that they have no competing financial interests.

Correspondence and requests for materials should be addressed to D.A.A. (e-mail: agard@msg.ucsf.edu).